

Journal of Materials Chemistry A

Accepted Manuscript



This is an *Accepted Manuscript*, which has been through the Royal Society of Chemistry peer review process and has been accepted for publication.

Accepted Manuscripts are published online shortly after acceptance, before technical editing, formatting and proof reading. Using this free service, authors can make their results available to the community, in citable form, before we publish the edited article. We will replace this *Accepted Manuscript* with the edited and formatted *Advance Article* as soon as it is available.

You can find more information about *Accepted Manuscripts* in the [Information for Authors](#).

Please note that technical editing may introduce minor changes to the text and/or graphics, which may alter content. The journal's standard [Terms & Conditions](#) and the [Ethical guidelines](#) still apply. In no event shall the Royal Society of Chemistry be held responsible for any errors or omissions in this *Accepted Manuscript* or any consequences arising from the use of any information it contains.



www.rsc.org/materialsA

COMMUNICATION

Highly Efficient Fullerene/Perovskite Planar Heterojunction Solar Cells via Cathode Modification with an Amino-Functionalized Polymer Interlayer

Cite this: DOI: 10.1039/x0xx00000x

Received 00th January 2012,
Accepted 00th January 2012

DOI: 10.1039/x0xx00000x

www.rsc.org/

Qifan Xue,^{†,a} Zhicheng Hu,^{†,a} Jiang Liu,^b Jiahui Lin,^b Chen Sun,^a Ziming Chen,^a Chunhui Duan,^a Jing Wang,^a Cheng Liao,^b Woon Ming Lau,^b Fei Huang,^{*,a} Hin-Lap Yip^{*,a} and Yong Cao^a

A new amino-functionalized polymer, PN4N, was developed and applied as an efficient interlayer to improve the cathode interface of fullerene/perovskite (CH₃NH₃PbI_xCl_{3-x}) planar heterojunction solar cells. The PN4N polymer is soluble in IPA and n-BuOH, which are orthogonal solvents to the metalhalide perovskite films and therefore can be spuncast on the heterojunction layer before the deposition of the metal cathode. Such a simple modification of the cathode interface showed a remarkable enhancement of power conversion efficiency (PCE) from 12.4% to 15.0% and also reduced the hysteresis of photocurrent. We also found that conventional water/methanol-soluble polymer interlayer, such as PFN, was incompatible with the perovskite films as the small molecular size, aprotic solvent such as MeOH could decompose the perovskite films to PbI₂, resulted in much lower solar cell performance. This study provides new design guidelines for efficient interfacial materials and also demonstrated that interface engineering could be a key strategy to improve perovskite solar cells.

Introduction

Solar cells based on halide perovskites (e.g. CH₃NH₃PbX₃, X = I, Cl, Br) as light absorbers are emerging as a low-cost and high performance photovoltaic technology that may fulfill the requirements for large-scale deployment of solar energy. Recent studies revealed that organometal trihalide perovskites exhibit several desired properties for photovoltaic applications including high absorption coefficient,¹ low exciton binding energy,^{1, 2} long carrier-diffusion lengths and facile tunable bandgaps,^{1, 3, 4} enabling their efficiencies leap from less than 5% to over 17% in the past 5 years.⁵⁻¹⁶

A typical perovskite solar cell composes of a light harvesting perovskite layer sandwiched between a transparent electrode and a

metal electrode. Charge selective interlayers are usually required to improve the charge extraction property and determine the polarity of the perovskite solar cells.^{17, 18} One of the major advantages of perovskite solar cells is that they can be fabricated with low-cost and simple solution processes. The perovskite semiconductor films can be simply prepared from precursor solutions containing mixed alkylammonium halides and metal halides through a one-step deposition method, though other deposition methods such as 2-step subsequent processing and vacuum deposition can also result in high performance devices.^{11, 19} The perovskite semiconductors can also be adopted in various types of solar cell architectures including perovskite-sensitized solar cells,²⁰ meso-superstructured solar cells and planar p-i-n heterojunction solar cells.^{8, 10} The latter one, which has a device architecture resembles that of polymer solar cells, is particularly attractive for potential commercialization due to the simplicity of the device structure, the low-temperature solution processibility and the potential of large-scale manufacturing of the perovskite cells using a continuous coating technique on flexible substrates.^{10, 21-25}

In addition to the control of crystallization process and morphology of the perovskite films,^{19, 26-29} the introduction of proper interfacial materials to optimize the electronic and electrical properties between the interfaces of the light-harvesting perovskite layer and the charge-collecting electrode is another important criterion to improve perovskite solar cell performances.^{15, 30-32} Seok *et al* systematically studied the interface between perovskite and a series of triarylamine polymer derivatives with different highest occupied molecular orbital (HOMO) levels and found that energetically favorable contact can help to maximize the voltage output.³³ In the case of fullerene/perovskite planar heterojunction solar cells, the application of ICBA significantly increased the V_{oc} and the PCE of the perovskite solar cells when compared to that based on PCBM. Thermally evaporated C₆₀/BCP double layer and

thin LiF layer as well as the solution-processed fullerene and polymer surfactant could also modify the cathode contact and realize efficient perovskite solar cells.^{13, 22, 23, 28, 32, 34-36}

Conjugated polymer electrolytes (CPEs) are another class of efficient interfacial materials that had been extensively used to improve the cathode interface in polymer solar cells.³⁷ A classic example is a water/methanol soluble polyfluorene derivative, PFN, which contains side chain terminated with alkylamines.³⁷⁻³⁹ It was found that the CPE interlayer can improve the solar cell performance in multiple ways, which includes the formation of appropriate dipoles for better energy level alignment at the electrode/active layer interface;^{38, 39} the improvement of electron selectivity at the cathode by efficiently blocking holes;⁴⁰ and also the improvement of interfacial charge transport properties.^{17, 18, 43} Motivated by the excellent interfacial properties offered by the CPEs, it is worth to introduce CPE interlayers to improve perovskite-based solar cells. However, one of the criteria for successfully applying CPEs interlayer to perovskite cells is that the CPEs should possess orthogonal solvent processibility to the perovskite film. Conventional CPEs that processed from methanol or aqueous solution will not be suitable as the highly polar solvents can dissolve and degrade the perovskite films. Therefore, the development of new CPE interfacial materials with compatible processibility to the perovskite films is needed for constructing multilayer solution-processed perovskite solar cells.

Here we report a remarkable enhancement of perovskite solar cell efficiencies by introducing a new amino-functionalized polymer, PN4N, as a novel cathode interlayer in a device structure of ITO/PEDOT:PSS/perovskite/PC₆₁BM/Interlayer/Al (See Fig. 1a). The newly designed PN4N can be processed from isopropyl alcohol (IPA), which is an orthogonal solvent to the perovskite film and therefore can be directly deposited from solution without corroding the perovskite underlayer film. This simple interfacial modification

strategy resulted in reduction of the contact resistance, suppression of bimolecular recombination, and also improvement of electron transport in the device, which led to an enhancement of PCE from 12.4% to 15.0%. Solar cells based on conventional PFN interlayer were also prepared but the performance was decreased due to the incompatibility of the processing solvent, which degraded the perovskite films.

Results and discussion

The chemical structures of PN4N and PFN are shown in Fig. 1a. Compares with PFN, which has a backbone composes of alternating rigid fluorene blocks with alkyl- and alkylamine-substituted side chains, a flexible amine-functionalized aliphatic segment was introduced into the PN4N backbone. This simple modification enables the PN4N polymer to be soluble in a wide range of alcoholic solvents. PFN has a relatively poor solubility and it can only be dissolved in methanol after quaternization of the amine groups. PN4N was prepared via Suzuki coupling reaction from monomers M1 and M2 with the presence of palladium catalyst.⁴¹ The synthetic procedure for PN4N is shown in Scheme 1 and the details can be found in the supporting information.

The perovskite films were prepared by one-step spincoating of the precursor solution composed of lead halides and methylammonium iodides in DMF followed by thermal annealing to promote crystallization of the perovskites. The top-view scanning electron microscopy (SEM) image shown in Fig. 1b revealed that perovskite film with high coverage of ~97% was formed on the PEDOT:PSS film. PCBM with a thickness of ~80 nm was used as an electron transport layer. Before vacuum deposition of the Al cathode, PFN and PN4N interlayer were spincoated on PCBM from MeOH and IPA, respectively. The cross-section SEM image of the PN4N-modified solar cell (Fig. 1c) showed that a well-defined layer-by-layer structure was formed. The thickness of the perovskite films used in our study was ~450 nm and the grain size was up to ~1 μm.

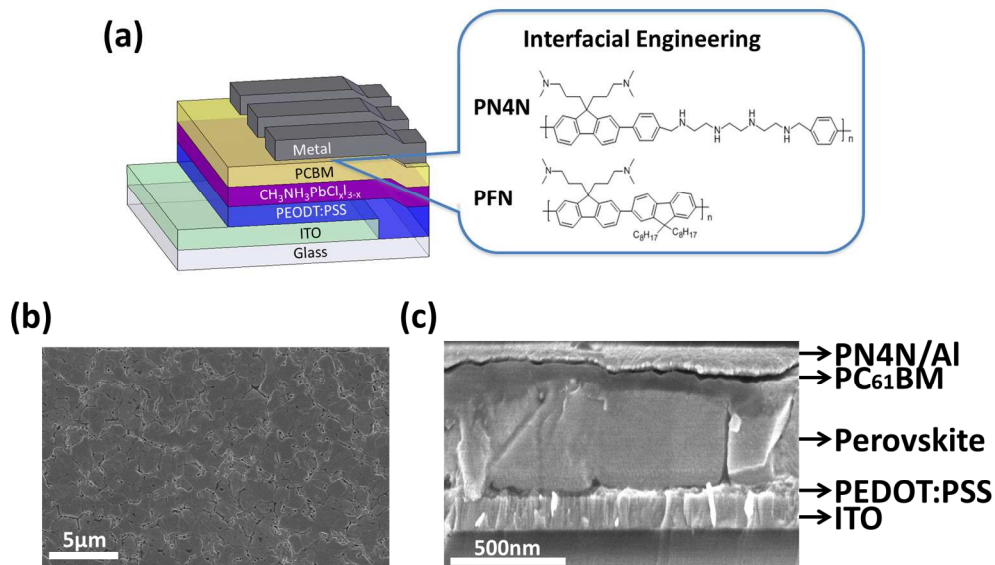
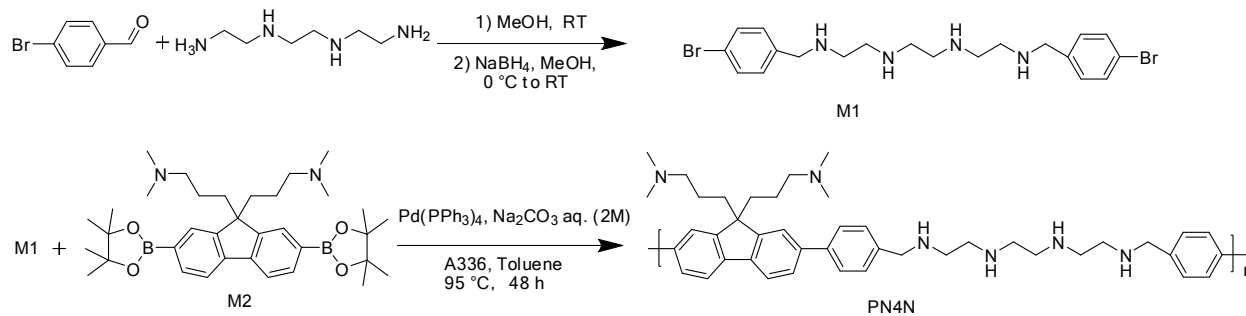


Fig. 1. (a) Device structure of the hybrid planar heterojunction solar cell and the molecular structure of PN4N and PFN; (b) Top-view SEM image of perovskite film on ITO/PEDOT:PSS substrate and (c) cross-section SEM image of the planar heterojunction perovskite solar cell.



Scheme 1 . Synthetic procedures for PN4N.

Table 1. The photovoltaic parameters of perovskite solar cells with different cathode modifications (under 100 mW cm⁻² air mass 1.5 global (AM 1.5 G) illumination).

Cathode	V _{oc} (V)	J _{sc} (mA/cm ²)	FF(%)	PCE(%)	R _s (Ωcm ²)	R _p (Ωcm ²)
Al	0.97	20.40	62.5	12.4	7.5	612.3
PN4N/Al	1.00	20.61	72.5	15.0	6.7	812.4
IPA/Al	0.98	20.47	62.1	12.5	7.3	602.5
PFN/Al	0.89	17.76	55.2	8.7	6.5	491.5
MeOH/Al	0.85	17.15	53.8	7.8	7.9	400.5

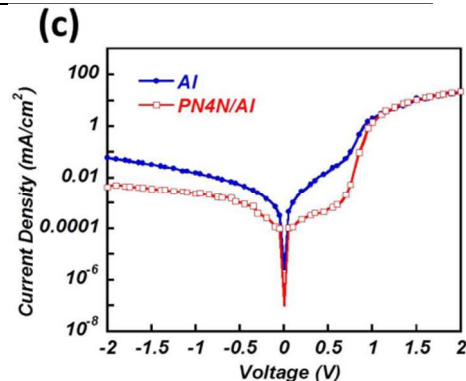
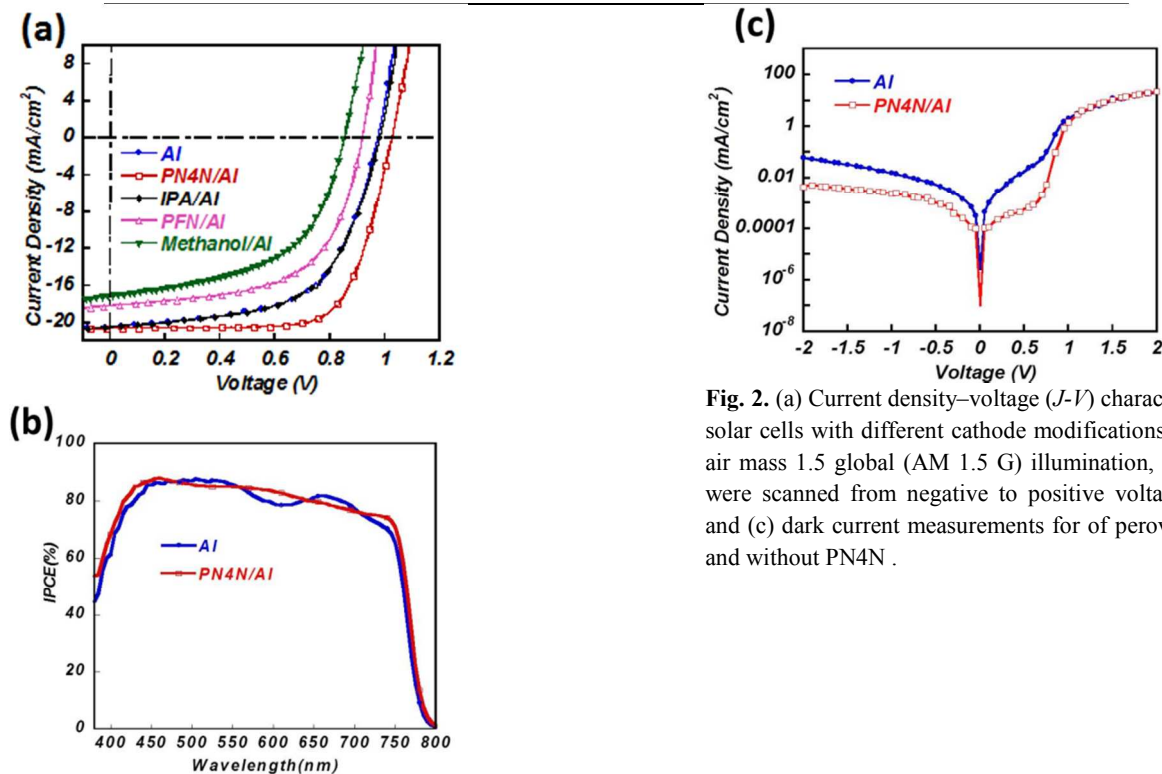


Fig. 2. (a) Current density–voltage (J - V) characteristics of perovskite solar cells with different cathode modifications under 100 mWcm⁻² air mass 1.5 global (AM 1.5 G) illumination, all the measurements were scanned from negative to positive voltage. (b) IPCE spectra and (c) dark current measurements for of perovskite solar cells with and without PN4N .

The solar cell performance measured under 100 mW cm^{-2} air mass 1.5 global (AM 1.5 G) illumination are summarized in Table 1 and the current density versus voltage ($J-V$) plots are shown in Fig. 2. The optimized control devices with an Al cathode delivered a PCE of 12.4% with V_{oc} , J_{sc} and FF equal to 0.97 V, 20.40 mA/cm^2 and 0.625, respectively. Incorporation of a PN4N interlayer with thickness of 5 nm led to simultaneous increase in all solar cell parameters with a V_{oc} of 1.00 V, J_{sc} of 20.61 mA/cm^2 and FF of 0.725, resulted in a significant improvement in PCE by $\sim 20\%$ over the control devices. The average PCEs of the devices achieved with and without the PN4N/Al bilayer cathode were of 13.9% and 11.2%, respectively, and the statistic distributions of the cell performance are shown in Figure S1. The incident photon to electron conversion efficiency (IPCE) spectra for the solar cells with an Al cathode and a PN4N/Al bilayer cathode are shown in Figure 2b. The shape and magnitude of the IPCE spectra for both the cells are quite similar and both showed an average IPCE close to 80%, this is also in good agreement with the similar value of J_{sc} s obtained from the two different cells.

The major contribution to the improvement of PCE is from the significant improvement in FF in the case of PN4N-modified cells. Since the FF is governed by both the shunt resistance (R_p) and parasitic series resistance (R_s) of the solar cell, therefore those parameters were extracted from the $J-V$ curves for further analysis and the resistance data are provided in Table 1. The solar cells modified with a thin PN4N layer (5 nm) showed an obvious increase in R_p from 612.3 Ωcm^2 to 812.4 Ωcm^2 and also a decrease in R_s from 7.5 Ωcm^2 to 6.7 Ωcm^2 compared to the control devices. Since the loss of charge carriers through leakage paths in the films and the recombination of carriers during their transit through the cell will both affect the R_p , we therefore studied the electrical behavior of the devices in the dark and the corresponding $J-V$ curves are shown in Fig 2c. The dark current density of the solar cells with PN4N/Al bilayer cathode under reverse bias was about one order of magnitude smaller than that with bare Al cathode, suggesting that the modified interface can reduce leakage current at the cathode electrode. It is also possible that the interfacial modification can reduce the recombination of charges at the cathode interface by removing the trap states at the PCBM/metal interface and improve electron transport in the device by reducing the injection barrier between the PCBM and the metal electrode, which was reported in the case of polymer solar cells.^{17, 18, 38-40, 42, 43}

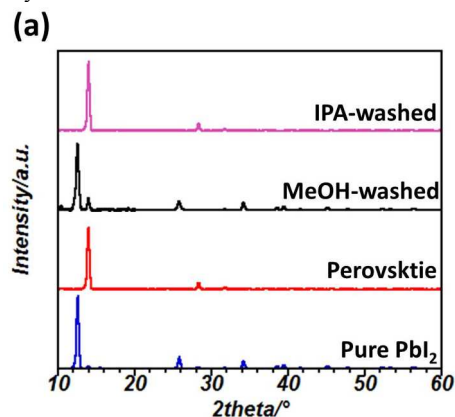
As a result, the reduction of both contact resistant at the cathode and the improved charge transport property of PCBM attribute to the decrease in R_s , leading to a significant improvement in FF and PCE of the modified solar cells. It is worth to note that there is an optimized thickness for the PN4N layer at ~ 5 nm, when the thickness further increases, the device performance decreased due to the resistance contributed from the interfacial layer. (Fig S2)

Photocurrent hysteresis originated from the presence of traps, ferroelectric respond in perovskite materials and the ion migration in the perovskite films and interlayers was observed in some perovskite solar cells.^{44, 45} However, devices with negligible photocurrent hysteresis could also be realized in the case of perovskite/fullerene planar heterojunction solar cells provided that optimized perovskite films and interfaces were achieved.^{13, 35, 36, 46, 47} We therefore also tested hysteresis property for the PN4N-modified perovskite cells by sweeping the $J-V$ measurement from both forward and reversed direction and we observed insignificant hysteresis in our devices with smaller than 1% difference in PCE. (Fig. S3). We attributed this to the good quality perovskite film with high coverage and also the improved cathode interface with PN4N modification.

In addition to the PN4N, a commonly used conjugated polymer electrolyte, PFN, was also applied as the interfacial layer for the

perovskite solar cells. The PCE of the PFN-modified solar cells dropped significantly from 12.4% of the reference cell to 8.7% (Fig 2a and Table 1), with all the three photovoltaic parameters decreased simultaneously. When the PFN solution was allowed to stay on the PCBM film for longer time of 60s before spin coating, the devices showed no obvious photovoltaic effect and the film was turned from dark brown to yellowish. (see Fig. S4) Since the major difference between the processing of PN4N and PFN films was the choice of solvents, that led us to also study the processing solvent effect on the perovskite solar cells. Devices fabricated by spincoating pure MeOH and IPA solvents on top of the PCBM layer before the deposition of Al electrode were tested and the results are shown in Fig 2a and Table 1. The IPA-washed devices showed photovoltaic characteristics equal to that of the reference devices while the MeOH-washed devices showed a significant drop in PCE to less than 8%. These results suggested that the solvent can significantly affect the quality of the perovskite film. To further study the effect of different solvents on the perovskite films, the films were washed by a series of alcoholic solvents including MeOH, EtOH, IPA and n-BuOH and the photographs of the washed films were shown in Fig. S5. The color of the perovskite films remained dark brown when washed by the IPA and n-BuOH but they turned into yellowish when washed by the MeOH and EtOH, indicating that the perovskite structure was broken down and only the yellowish PbI_2 was left behind. We suggested that aprotic solvents like MeOH and EtOH are small enough to penetrate into the perovskite crystal lattice and break down the ionic interactions between the CH_3NH_3^+ and PbI_3^- framework, and eventually washing out the $\text{CH}_3\text{NH}_3\text{I}$. IPA and n-BuOH are larger in size and therefore more difficult to break down the perovskite crystal structure, making them a good orthogonal solvent to the perovskite films.

X-ray diffraction (XRD) and absorbance spectra studies were further used to investigate the effect of different solvents on perovskite crystal structure (Fig. 3). Pristine perovskite films showed strong peaks at $2\theta = 14.0^\circ$, 28.2° and 31.6° , which correspond to the (110), (220) and (310) planes, respectively, and are consistent with the previously reported perovskite crystal structure.^{6, 20, 48-50} An additional strong peak at 12.65° corresponding to the phase of PbI_2 was found when the perovskite film was washed by MeOH while the XRD spectrum remained identical to the reference film when the film was washed by IPA. In the meanwhile, perovskite film washed by MeOH exhibited similar absorbance spectra to PbI_2 while perovskite film washed by IPA showed identical absorption spectra to the pristine film. Based on the results of the optical images, XRD and absorbance spectra, we conclude that solvents with small molecular sizes (e.g. MeOH, EtOH) deteriorate the perovskite crystal structure and decompose it to PbI_2 while solvents with larger molecular sizes (e.g. IPA, n-BuOH) have little effect on the perovskite crystal structure.



COMMUNICATION

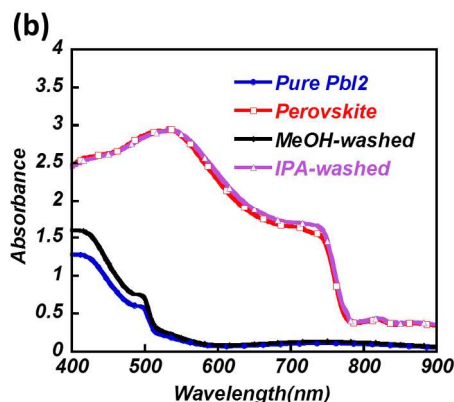


Fig. 3. (a) XRD patterns and (b) UV-vis absorption spectra of PbI_2 film, perovskite films with and without being washed by MeOH and IPA.

Conclusion

We have successfully demonstrated highly efficient planar heterojunction perovskite solar cells through the introduction of a newly developed amino-functionalized polymer, PN4N, as an efficient cathode interlayer. This charge selective PN4N interlayer led to reduction of the contact resistance, suppression of interfacial charge recombination, and also improvement of the electron transport property of the perovskite solar cells and therefore resulted

Notes and references

- C. C. Stoumpos, C. D. Malliakas and M. G. Kanatzidis, *Inorg. Chem.*, 2013, **52**, 9019-9038.
- H. J. Snaith, *J. Phys. Chem. Lett.*, 2013, **4**, 3623-3630.
- J. H. Noh, S. H. Im, J. H. Heo, T. N. Mandal and S. I. Seok, *Nano Lett.*, 2013, **13**, 1764-1769.
- F. Hao, C. C. Stoumpos, R. P. H. Chang and M. G. Kanatzidis, *J. Am. Chem. Soc.*, 2014, **136**, 8094-8099.
- H. S. Kim, C. R. Lee, J. H. Im, K. B. Lee, T. Moehl, A. Marchioro, S. J. Moon, R. Humphry-Baker, J. H. Yum, J. E. Moser, M. Graetzel and N. G. Park, *Sci. Rep.*, 2012, **2**, 591-597.
- J.-H. Im, C.-R. Lee, J.-W. Lee, S.-W. Park and N.-G. Park, *Nanoscale*, 2011, **3**, 4088-4093.
- M. M. Lee, J. Teuscher, T. Miyasaka, T. N. Murakami and H. J. Snaith, *Science*, 2012, **338**, 643-647.
- J. M. Ball, M. M. Lee, A. Hey and H. J. Snaith, *Energy Environ. Sci.*, 2013, **6**, 1739-1743.
- M. Liu, M. B. Johnston and H. J. Snaith, *Nature*, 2013, **501**, 395-398.
- D. Liu and T. L. Kelly, *Nat Photon*, 2014, **8**, 133-138.
- K. Wojciechowski, M. Saliba, T. Leijtens, A. Abate and H. J. Snaith, *Energy Environ. Sci.*, 2014, **7**, 1142-1147.
- M. He, D. Zheng, M. Wang, C. Lin and Z. Lin, *J. Mater. Chem. A*, 2014, **2**, 5994-6003.
- Q. Wang, Y. Shao, Q. Dong, Z. Xiao, Y. Yuan and J. Huang, *Energy Environ. Sci.*, 2014, **7**, 2359-2365.
- N. N. R. E. L. (NREL), www.nrel.gov/ncpv/images/efficiency_chart.jpg.
- H. Zhou, Q. Chen, G. Li, S. Luo, T.-b. Song, H.-S. Duan, Z. Hong, J. You, Y. Liu and Y. Yang, *Science*, 2014, **345**, 542-546.
- A. Kojima, K. Teshima, Y. Shirai and T. Miyasaka, *J. Am. Chem. Soc.*, 2009, **131**, 6050-6051.
- H.-L. Yip and A. K. Y. Jen, *Energy Environ. Sci.*, 2012, **5**, 5994-6011.
- T. Yang, M. Wang, C. Duan, X. Hu, L. Huang, J. Peng, F. Huang and X. Gong, *Energy & Environmental Science*, 2012, **5**, 8208-8214.
- J. Burschka, N. Pellet, S.-J. Moon, R. Humphry-Baker, P. Gao, M. K. Nazeeruddin and M. Graetzel, *Nature*, 2013, **499**, 316-319.
- A. Kojima, K. Teshima, Y. Shirai and T. Miyasaka, *J. Am. Chem. Soc.*, 2009, **131**, 6050-6051.
- J. You, Z. Hong, Y. Yang, Q. Chen, M. Cai, T.-B. Song, C.-C. Chen, S. Lu, Y. Liu, H. Zhou and Y. Yang, *Acs Nano*, 2014, **8**, 1674-1680.
- J.-Y. Jeng, Y.-F. Chiang, M.-H. Lee, S.-R. Peng, T.-F. Guo, P. Chen and T.-C. Wen, *Adv. Mater.*, 2013, **25**, 3727-3732.
- J. Y. Jeng, K. C. Chen, T. Y. Chiang, P. Y. Lin, T. D. Tsai, Y. C. Chang, T. F. Guo, P. Chen, T. C. Wen and Y. J. Hsu, *Adv Mater*, 2014, **26**, 4107-4113.
- S. Sun, T. Salim, N. Mathews, M. Duchamp, C. Boothroyd, G. Xing, T. C. Sum and Y. M. Lam, *Energy Environ. Sci.*, 2014, **7**, 399-407.
- P. Docampo, J. M. Ball, M. Darwich, G. E. Eperon and H. J. Snaith, *Nat Commun*, 2013, DOI:10.1038/ncomms3761.
- G. E. Eperon, V. M. Burlakov, P. Docampo, A. Goriely and H. J. Snaith, *Adv. Funct. Mater.*, 2014, **24**, 151-157.
- Y. Wu, A. Islam, X. Yang, C. Qin, J. Liu, K. Zhang, W. Peng and L. Han, *Energy Environ. Sci.*, 2014, **7**, 2934-2938.

in a remarkable enhancement of PCE from 12.4% to 15.0%. In addition, we have studied the dependence of perovskite crystal structure on the interlayer processing solvents and found that small size aprotic solvents (e.g. MeOH, EtOH) can destroy the perovskite crystal structure and solvents with larger molecular sizes (e.g. IPA, n-BuOH) has little effect on perovskite crystal structure. This study provides new design guidelines for efficient interfacial materials and device process for high performance perovskite solar cells.

Acknowledgements

This work was financially supported by the Ministry of Science and Technology of the People's Re (No. 2014CB643505), the Natural Science Foundation of China (No. 51323003 and 21125419), and the Guangdong Natural Science Foundation (No. S2012030006232).

^a Institute of Polymer Optoelectronic Materials and Devices, State Key Laboratory of Luminescent Materials and Devices, South China University of Technology, Guangzhou 510640, P. R. China.

^b Chengdu Green Energy and Green Manufacturing Technology R&D Centre, Southwest Airport Economic Development Zone, Shuangliu, Chengdu, 610207, P. R. China.

† These authors contributed equally to this work.

28. P.-W. Liang, C.-Y. Liao, C.-C. Chueh, F. Zuo, S. T. Williams, X.-K. Xin, J. Lin and A. K. Y. Jen, *Adv. Mater.*, 2014, **26**, 3748-3754.
29. Z. Wu, S. Bai, J. Xiang, Z. Yuan, Y. Yang, W. Cui, X. Gao, Z. Liu, Y. Jin and B. Sun, *Nanoscale*, 2014, **6**, 10505-10510.
30. K.-G. Lim, H.-B. Kim, J. Jeong, H. Kim, J. Y. Kim and T.-W. Lee, *Adv. Mater.*, 2014, DOI: 10.1002/adma.201401775.
31. J. H. Heo, S. H. Im, J. H. Noh, T. N. Mandal, C.-S. Lim, J. A. Chang, Y. H. Lee, H.-j. Kim, A. Sarkar, M. K. Nazeeruddin, M. Graetzel and S. I. Seok, *Nature Photonics*, 2013, **7**, 487-492.
32. H. Zhang, H. Azimi, Y. Hou, T. Ameri, T. Przybilla, E. Spiecker, M. Kraft, U. Scherf and C. J. Brabec, *Chem. Mater.*, 2014, DOI: 10.1021/cm502864s.
33. S. Ryu, J. H. Noh, N. J. Jeon, Y. Chan Kim, W. S. Yang, J. Seo and S. I. Seok, *Energy Environ. Sci.*, 2014, **7**, 2614-2618.
34. Z. Xiao, C. Bi, Y. Shao, Q. Dong, Q. Wang, Y. Yuan, C. Wang, Y. Gao and J. Huang, *Energy Environ. Sci.*, 2014, **7**, 2619-2623.
35. J. W. Seo, S. Park, Y. C. Kim, N. J. Jeon, J. H. Noh, S. C. Yoon and S. I. Seok, *Energy Environ. Sci.*, 2014, **7**, 2642-2646.
36. P.-W. Liang, C.-C. Chueh, X.-K. Xin, F. Zuo, S. T. Williams, C.-Y. Liao and A. K. Y. Jen, *Adv. Energy Mater.*, 2014, DOI:10.1002/aenm.201400960.
37. C. Duan, K. Zhang, C. Zhong, F. Huang and Y. Cao, *Chem. Soc. Rev.*, 2013, **42**, 9071-9104.
38. Z. He, C. Zhong, S. Su, M. Xu, H. Wu and Y. Cao, *Nat. Photonics*, 2012, **6**, 591-595.
39. Z. C. He, C. Zhang, X. F. Xu, L. J. Zhang, L. Huang, J. W. Chen, H. B. Wu and Y. Cao, *Adv. Mater.*, 2011, **23**, 3086-3089.
40. C. Duan, W. Cai, B. B. Hsu, C. Zhong, K. Zhang, C. Liu, Z. Hu, F. Huang, G. C. Bazan and A. J. Heeger, *Energy Environ. Sci.*, 2013, **6**, 3022-3034.
41. H. Wang, P. Lu, B. Wang, S. Qiu, M. Liu, M. Hanif, G. Cheng, S. Liu and Y. Ma, *Macromol Rapid Comm*, 2007, **28**, 1645-1650.
42. H.-L. Yip, S. K. Hau, N. S. Baek, H. Ma and A. K. Y. Jen, *Adv. Mater.*, 2008, **20**, 2376-2382.
43. Z. C. He, C. M. Zhong, X. Huang, W. Y. Wong, H. B. Wu, L. W. Chen, S. J. Su and Y. Cao, *Adv. Mater.*, 2011, **23**, 4636-4643.
44. H. J. Snath, A. Abate, J. M. Ball, G. E. Eperon, T. Leijtens, N. K. Noel, S. D. Stranks, J. T.-W. Wang, K. Wojciechowski and W. Zhang, *J. Phys. Chem. Lett.*, 2014, **5**, 1511-1515.
45. E. L. Unger, E. T. Hoke, C. D. Bailie, W. H. Nguyen, A. R. Bowring, T. Heumuller, M. G. Christoforo and M. D. McGehee, *Energy Environ. Sci.*, 2014, DOI: 10.1039/c1034ee02465f.
46. Z. Xiao, C. Bi, Y. Shao, Q. Dong, Q. Wang, Y. Yuan, C. Wang, Y. Gao and J. Huang, *Energy Environ. Sci.*, 2014.
47. Z. Xiao, C. Bi, Y. Shao, Q. Dong, Q. Wang, Y. Yuan, C. Wang, Y. Gao and J. Huang, *Energy Environ. Sci.*, 2014, **7**, 2619-2623.
48. D. Bi, S.-J. Moon, L. Haggman, G. Boschloo, L. Yang, E. M. J. Johansson, M. K. Nazeeruddin, M. Graetzel and A. Hagfeldt, *Rsc Advances*, 2013, **3**, 18762-18766.
49. Y. Zhao, A. M. Nardes and K. Zhu, *J. Phys. Chem. Lett.*, 2014, **5**, 490-494.
50. N.-G. Park, *J. Phys. Chem. Lett.*, 2013, **4**, 2423-2429.

COMMUNICATION

ToC

